In Situ Atomic Oxygen Erosion Study of Fluoropolymer Films Using X-ray Photoelectron Spectroscopy

Rene I. Gonzalez,[1] Shawn H. Phillips,[1] Gar B. Hoflund[2]

[1]*Propulsion Materials Applications Branch, Air Force Research Laboratory, Edwards Air Force Base, California 93524*
[2]*Department of Chemical Engineering, University of Florida, Gainesville, Florida 32611*

Received 7 July 2003; accepted 3 October 2003

ABSTRACT: The surfaces of a homologous series of fluoropolymers were characterized *in situ* using X-ray photoelectron spectroscopy before and after a 15-min exposure to the flux produced by a unique hyperthermal atomic oxygen (AO) source, which produces a flux of about of 10^{15} atoms cm^{-2} s^{-1}. The linear polymers investigated in this study include high-density polyethylene (HDPE), poly(vinyl fluoride) (PVF), poly(vinylidene fluoride) (PVdF), and poly(tetrafluoroethylene) (PTFE). They possess a similar base structure with increasing fluorine-to-carbon ratios of 0, 1 : 2, 1 : 1, and 2 : 1, respectively. No interaction of the AO with the nonfluorine-containing linear polymer HDPE was detected over this short exposure. However, a correlation exists between the chemical composition of the fluorinated polymers and the induced chemical and structural alterations occurring in the near-surface region as a result of exposure to AO. The data indicate that AO initially attacks the fluorine portion of the polymers, resulting in a substantial decrease in the near-surface fluorine concentration. The near-surface fluorine-to-carbon ratios of PVF, PVdF, and PTFE decreased during the 15-min AO exposure by 68, 39, and 18.5%, respectively. © 2004 Wiley Periodicals, Inc. J Appl Polym Sci 92: 1977–1983, 2004

Key words: atomic oxygen; low earth orbit (LEO); polymer, space, fluorine, fluoropolymers

INTRODUCTION

Polymers are attractive and desirable materials for use in space applications because they are lightweight and are typically much easier to process using techniques such as extrusion, casting, and injection molding at temperatures relatively lower than those used for metals and ceramics. They also tend to be more flexible and offer a wide variety of choices from optically transparent to opaque, rubbery to stiff, and conducting to insulating. However, over the last two decades, it has been well established that polymers undergo severe degradation, resulting in reduced spacecraft lifetimes. These materials degrade because spacecraft surfaces are exposed to high fluxes of atomic oxygen (AO), bombardment by low- and high-energy charged particles, thermal cycling, and the full spectrum of solar radiation. AO is the main constituent of the atmosphere in low earth orbit (LEO) and is formed by the dissociation of molecular oxygen by ultraviolet radiation from the sun, resulting in an AO concentration of approximately 10^8 atoms/cm^3. The reverse reaction in which an oxygen molecule forms from AO does not have a high reaction rate because it requires a teratomic collision. The third atom is required to dissipate the energy released by formation of O_2. The actual flux of about 10^{15} atoms cm^{-2} s^{-1} impinging on a spacecraft is high because of orbiting speeds of approximately 8 km/s. At these relative speeds thermal AO collides with a kinetic energy of about 5 eV. These highly energetic collisions not only result in surface chemical reactions but can also lead to a pure physical sputtering of the surface atoms in the absence of any chemical changes. Many studies have been conducted in an effort to determine the mechanism of this degradation primarily caused by surface reactions with AO.[1–8] However, these studies have all been carried out after exposing these highly reactive surfaces to air before analysis, thus introducing artifacts that do not represent the true space environment. Recent studies have shown that exposure to air chemically alters the reactive surfaces formed during AO exposure.[9,10] It is therefore essential that analysis of polymers exposed to AO be carried out *in situ* to avoid artifacts induced by air exposure. An understanding of how AO alters polymer surfaces will aid in the development of new materials with acceptable erosion properties.

Recently, several polymer systems were characterized *in situ* using X-ray photoelectron spectroscopy (XPS) before and after incremental exposures to the flux produced by an electron-stimulated desorption (ESD) AO source.[11–13] These studies showed that polymers containing polyhedral oligomeric silsesquioxane (POSS) moieties rapidly form a passivating silica layer

Correspondence to: G. Hoflund (hoflund@che.ufl.edu).
Contract grant sponsor: AFOSR; contract grant number: F49620-01-0338.

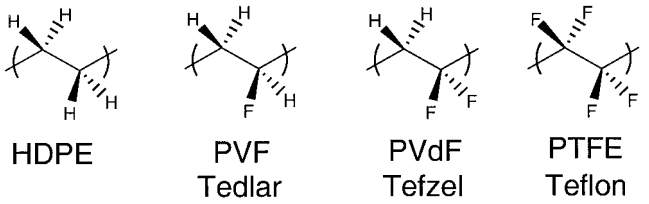

Figure 1 Chemical structures of the polymers used in this study.

that serves as a protective barrier preventing further degradation of the underlying polymer with increased exposure to the AO flux. In this study, a series of fluoropolymer films was investigated in an effort to further understand AO-induced surface alterations of different polymer systems and to establish a basis for comparison in future POSS-fluorinated polymer studies. The polymers chosen for this study (Fig. 1) include Tedlar [poly(vinyl fluoride) (PVF)], Tefzel [poly(vinylidene fluoride) (PVdF)], and Teflon [poly(tetrafluoroethylene)] having fluorine-to-carbon ratios of 1 : 2, 1 : 1, and 2 : 1, respectively. High-density polyethylene (HDPE), which does not contain fluorine, was also examined. The study of these polymers with similar structure but increasing fluorine content indicates a correlation between chemical composition and induced chemical and structural alterations by AO exposure.

Several studies were conducted on the deterioration of fluorinated polymers retrieved from spacecraft subjected to the LEO environment. The outer layer of Teflon-fluorinated ethylene–propylene (FEP) multilayer insulation on the Hubble space telescope (HST) was significantly cracked at the time of the second HST-servicing mission, 6.8 years after it was launched into low earth orbit.[14,15] Comparatively minor embrittlement and cracking were also observed in the FEP materials retrieved from solar-facing surfaces on the HST at the time of the first servicing mission (3.6 years of exposure). Furthermore, an increased deterioration of fluorinated polymers results from the synergistic effect of VUV radiation in the presence of AO.[16] Thin films of fluorinated polymers such as Teflon–FEP are used as the outer layer of multilayer thermal control insulation because of their superior optical properties, including low solar absorbency and high thermal reflectance. A metallized layer is applied to the backside to reflect incident sunlight.[14]

EXPERIMENTAL

O-atom source characteristics

A schematic diagram illustrating the operational principles of the ESD AO source is shown in Figure 2(a). Ultrahigh-purity molecular oxygen dissociatively ad-

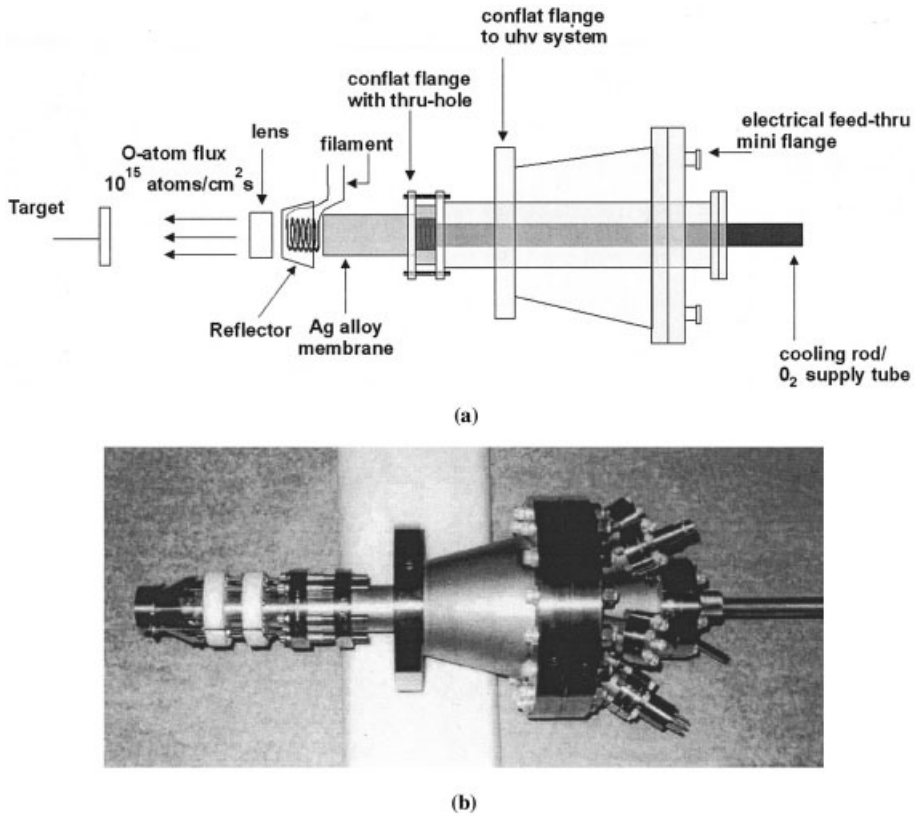

Figure 2 (a) Schematic diagram of the atomic oxygen source. (b) Photograph of atomic oxygen source.

sorbs on the high-pressure (2 Torr) side of a thin metallic Ag–alloy membrane maintained at elevated temperature (~ 400°C) and permeates through the membrane to the UHV side. There the chemisorbed atoms are struck by a directed flux of primary electrons, which results in ESD of the O atoms forming a continuous flux. The primary electrons are produced by thermionic emission from a coiled hot filament supported around the perimeter of the membrane. An electron reflector (lens assembly) surrounds the filament. It produces a potential field, which creates a uniform flux of electrons over the membrane surface. These primary electrons have a kinetic energy of 1000 eV and provide two functions: ESD of the O atoms and heating of the membrane surface. Another lens is placed between the reflector and the sample for removal of all charged particles including secondary electrons and O^+ and O^- ions produced during the ESD process.

Several processes have to function in series at sufficiently high rates for this system to work, including dissociative chemisorption of the molecular gas on the metal surface, permeation of atomic oxygen through the membrane, and formation of the neutral flux by ESD. Because these processes occur in series, the slowest one determines the magnitude of the AO flux. The sticking coefficient of O_2 on polycrystalline Ag (step 1) is fairly small (~ 0.001) so it is necessary to use a high pressure on the upstream side of the membrane. However, the permeation rate through the membrane is proportional to the reciprocal of the membrane thickness. This means that it is desirable to have a high pressure and a thin membrane, although this can lead to membrane failure. The ESD rate can be increased by increasing the primary electron current to the membrane, but this increases the temperature of the membrane and can result in evaporation of Ag, which is unacceptable.

The AO produced by this source has been shown to be hyperthermal (energies greater than 0.01 to 0.02 eV), but their energy distribution was not measured. Corallo et al.[17] measured the energy distribution of O ions emitted by ESD from a Ag(110) surface and found that this distribution has a maximum of about 5 eV and a full-width at half maximum of 3.6 eV. This ion energy distribution sets an upper bound for the neutral energy distribution because ESD neutrals are generally believed to be less energetic than ESD ions based on models of the ESD process. This point has been discussed often in the ESD literature but not actually demonstrated. Because neutral ESD species are difficult to detect, very few ESD studies of neutral species have appeared in the literature. The neutral atom flux was previously detected by using a quadrupole mass spectrometer[18,19] in the appearance potential (AP) mode to allow the atoms to be distinguished from residual gases and background gas products formed by collisions of the neutrals with the walls of the UHV system. In this experiment the ion acceleration potential was set at 0.0 V. Calibration studies have demonstrated that the ions entering the quadrupole section must have a minimum kinetic energy of 2.0 eV to reach the detector so the ESD neutrals detected have a minimum energy of 2.0 eV. Therefore, the hyperthermal AO produced by this ESD source have energies greater than 2 eV but possibly less than the ion energy distribution. Furthermore, these mass spectrometric experiments have shown that the AO-to-O^+ ratio is about 10^8 and that the O^+-to-O^- ratio is about 100.

Several approaches have been used to measure the magnitude of the hyperthermal AO flux and reasonable agreement was obtained between the various methods. The flux from the ESD AO source is approximately 2×10^{15} atoms cm^{-2} s^{-1}. One of the most reliable methods for flux determination is the measurement of a ZrO_2 film growth rate.[20] A Zr flux was generated by e-beam evaporation and the flux was calibrated using a quartz-crystal monitor. Based on the facts that stoichiometric ZrO_2 was produced and that no O_2 was present in the AO flux, the AO flux was calculated. By doubling the Zr flux, stochiometric ZrO was grown.[21] The AO flux was also determined by measuring the chemisorption rate of AO on polycrystalline Au using ion-scattering spectroscopy.[22] The flux determined using this method is in excellent agreement with that determined using the oxide growth rate method.

Surface characterization

As-received E.I. du Pont Nemours & Co. (Wilmington, DE) Teflon, Tedlar, Tefzel, and HDPE films were wiped with isopropanol and inserted into the UHV chamber (base pressure $< 1.3 \times 10^{-10}$ Torr). XPS measurements were performed using a double-pass cylindrical mirror analyzer (DPCMA; PHI Model 25-270AR). XPS survey spectra were taken in the retarding mode with a pass energy of 50 eV, and high-resolution XPS spectra were taken with a pass energy of 25 eV using Mg–K_α X-rays (PHI Model 04-151 X-ray source). Data collection was accomplished using a computer-interfaced, digital pulse-counting circuit[23] followed by smoothing with digital-filtering techniques.[24] The sample was tilted 30° off the axis of the DPCMA, and the DPCMA accepted electrons emitted into a cone 42.6 ± 6° off the DPCMA axis.

XPS spectra were first obtained from the as-entered, solvent-cleaned sample. The sample was then transferred into an adjoining UHV chamber that houses the ESD AO source by a magnetically coupled rotary/linear manipulator. There the surface was exposed to a hyperthermal AO flux and reexamined without air exposure after a total exposure time of 15 min. At no

TABLE I
Polymer Name, Binding Energies, F/C ratio and Structure

Polymer	Binding energy (eV) C1s 1	C1s 2	F1s	F : C
(a) Poly(ethylene), high density (HDPE) $[–CH_2—CH_2–]_n$	285.00	N/A	N/A	0
(b) Tedlar, poly(vinyl fluoride) (PVF) $[–CH_2—CHF–]_n$	285.74	287.91	686.94	1 : 2
(c) Tefzel, poly(vinyl fluoride) (PVdF) $[–CH_2—CF_2–]_n$	286.44	290.90	688.15	1 : 1
(d) Teflon, poly(tetrafluorethylene) (PTFE) $[–CF_2—CF_2–]_n$	292.48	N/A	689.67	2 : 1

time were the samples exposed to air after the initial insertion into the UHV chamber. The approximate normal distance between the sample face and source in this study was 15 cm, at which distance the flux was about 2.0×10^{15} atoms cm^{-2} s^{-1} for the instrument settings used. The sample was maintained at room temperature during the AO exposures with a temperature increase to 50°C attributed to exposure to the X-ray source during XPS data collection. The substrate temperature was determined using a chromel–alumel thermocouple. Polymer structural repeat units, F-to-C ratios, and reference binding energies (BE) used in this study are given in Table I.

RESULTS AND DISCUSSION

XPS survey spectra obtained from the as-received, solvent-wiped polymer films before and after the 15-min AO exposure are shown in Figure 3. The peak assignments shown in Figure 3 pertain to all eight spectra. The predominant peaks apparent in these spectra include the C1s for all the samples in addition to the F1s, F Auger (KLL), and F2s for the fluoropolymers. Significant changes in relative peak shapes and heights were observed for the C and F features in the fluoropolymers after the AO exposures. However, essentially no change was observed in the spectra of polyethylene as a result of the 15-min exposure to AO. Longer-term AO exposures to polyethylene do result in significant changes including chemisorption of O at the surface and alteration of the C chemical state.[25] Estimates of the near-surface compositions were made from the peak areas in the high-resolution spectra using published atomic sensitivity factors,[26] with the assumption of a homogeneous surface region. XPS probes the near-surface region of the sample and yields a weighted-average composition with the atomic layers near the surface being weighted more heavily because the photoemitted electrons from these layers have a lower probability of scattering inelastically. The sampling depth was about 4–6 nm, and about 10% of the signal originates from the outermost atomic layer.[27] This near-surface region is nonhomogeneous because the AO reacts with the outermost few atomic layers. Therefore, the region that reacts to the greatest extent with AO also makes the largest contribution to the XPS signal. This fact implies that XPS is an excellent technique for studying AO erosion of spacecraft materials. Even though the distribution functions involving the depth of chemical reactions in the near-surface region and the XPS determination of the weighted-average composition of the near-surface region are complex, the compositional values provide a trend that is indicative of the chemical alterations

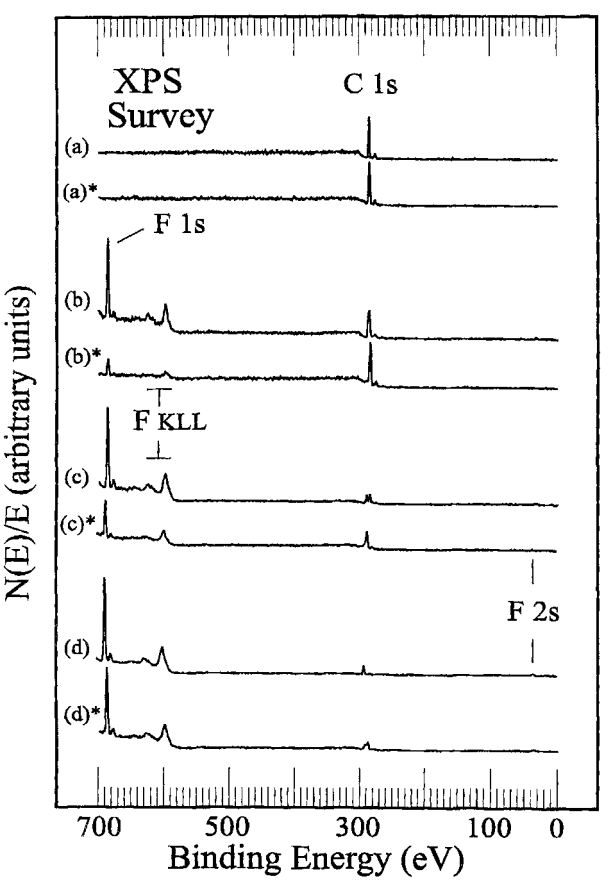

Figure 3 XPS survey spectra obtained from a solvent-cleaned, HDPE film after (a) insertion into the vacuum system (a*) 15-min AO exposure; PVF after (b) insertion into vacuum system, (b*) after 15-min AO exposure; PVdF after (c) insertion into vacuum system, (c*) after 15-min AO exposure; PTFE after (d) insertion into vacuum system, (d*) after 15-min AO exposure.

TABLE II
Near-Surface Composition (atomic %) Determined from XPS Data Obtained from the As-Entered, Solvent-Cleaned, and 15-min AO-Exposed HDPE and Fluoropolymer Samples

	Composition (at %)				F : C ratio		
	As-entered		15-min AO		Experimental		
Polymer surface	C	F	C	F	As-entered	15-min AO	Theoretical
HDPE $[–CH_2—CH_2–]_n$	100	0	100	0	0	0	0
PVF $[–CH_2—CHF–]_n$	69.2	30.8	86.2	13.8	0.89 : 2	0.32 : 2	1 : 2
PVdF $[–CH_2—CF_2–]_n$	52.1	47.9	62.1	37.9	0.92 : 1	0.61 : 1	1 : 1
PTFE $[–CF_2—CF_2–]_n$	34.2	65.8	38.0	62.0	1.92 : 2	1.63 : 2	2 : 1

occurring during AO exposure. The compositions determined using the homogeneous assumption are shown in Table II before and after the 15-min exposure to AO. No oxygen was detected in the survey spectra before and after exposure to AO. Both the spectra in Figure 3 and the data in Table II indicate that the F-to-C ratio decreases with AO exposure. The extent of this decrease is quite large for a short AO exposure. The extent was greatest for PVF and least for PTFE. The C—F bond was strong and thermal AO would not be expected to react with these polymers. The reduction in the F-to-C ratio was most likely attributable to selective physical sputtering of the F by the hyperthermal AO. Testing this assertion by using 5 eV Ne would be useful because this would induce no changes through chemical effects. In addition to relative peak size changes, peak shape changes are also apparent in Figure 3.

High-resolution XPS C1s and F1s spectra obtained from the as-received, solvent-wiped polymers before and after the 15-min AO exposures are shown in (a)–(d) and (a)–(c) of Figures 4 and 5, respectively. Variations in peak shapes and positions were observed between the nonexposed and AO-exposed fluoropolymer surfaces, indicating that the chemical species distribution was altered by exposure to the AO flux. No surface charging of the sample was evident during the experiment because this would have resulted in a significant BE shift. Differential charging would have manifested itself through peak broadening or peak multiplicity. However, this was not observed.

The C1s features shown in Figure 4 indicate that the predominant forms of carbon in the as-entered samples agree well with referenced BE values.[28] Each of these carbon species is in a different electrostatic environment and therefore exhibits a different chemical shift, producing C1s peaks in different positions in the spectrum. The C1s peak for aliphatic, hydrogen-saturated carbon of HDPE is broad and centered at 285.0 eV.[28] Carbon in the most electronegative environment (PTFE; Teflon) in Figure 4(d) appears at the highest BE of 292.5 eV. The electronegative fluorine atoms withdraw electron density from the valence and bonding orbitals of the carbon atom, thereby reducing the screening of the core electrons from the nuclear charge and increasing their BEs. No changes in the C chemical state were observed for the HDPE sample after the 15-min exposure to AO. However, significant reductions in the fluorinated carbon species were observed for the fluoropolymer films, which is consis-

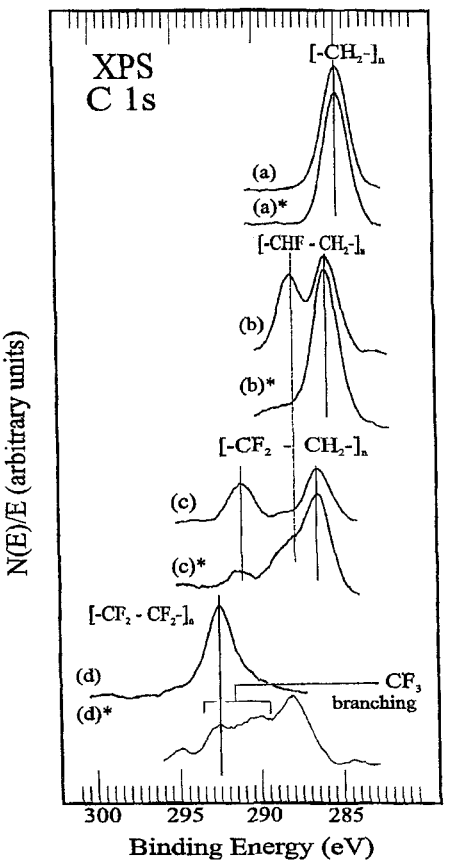

Figure 4 XPS C1s spectra obtained from a solvent-cleaned, HDPE film after (a) insertion into the vacuum system (a*) 15-min AO exposure; PVF after (b) insertion into vacuum system, (b*) after 15-min AO exposure; PVdF after (c) insertion into vacuum system, (c*) after 15-min AO exposure; PTFE after (d) insertion into vacuum system, (d*) after 15-min AO exposure.

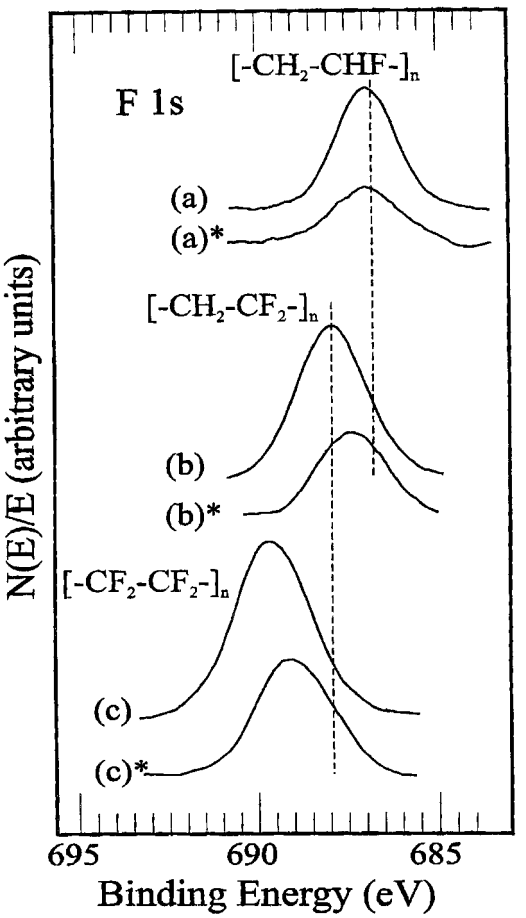

Figure 5 XPS F1s spectra obtained from a solvent-cleaned, PVF film after (a) insertion into vacuum system, (a*) after 15-min AO exposure; PVdF after (b) insertion into vacuum system, (b*) after 15-min AO exposure; PTFE after (c) insertion into vacuum system, (c*) after 15-min AO exposure.

tent with the reduced F-to-C ratios observed in Figure 3. In the C1s spectra for PVF (Tedlar) in Figure 4(b*), the peak corresponding to the monofluoro-substituted carbon (–CHF–), is essentially eliminated. This change coincides with a decrease in the total fluorine concentration in the near-surface region of 17 at %. The spectrum shown in Figure 4(c*) also reveals a substantial decrease in the peak corresponding to the difluoronated carbon species ($–CF_2–$) of PVdF (Tefzel) upon exposure to AO. This change coincides with a decrease in the total fluorine concentration in the near-surface region of 10 at %. However, a large shoulder develops at an approximate BE of 288 eV corresponding to the formation of the monofluoro-substituted carbon. Therefore, AO attacks Tedlar and Tefzel by cleaving off fluorine from the polymer backbone. AO reacts differently with PTFE (Teflon) resulting in $–CF_3$ branching as observed in Figure 4(d*). This probably results from scission of the polymer chain and subsequent loss of molecular weight and mechanical properties of the polymer. This is consistent with the results obtained from postdensity, NMR, and DSC analyses of the Teflon FEP samples retrieved from the HST.[14] The fact that F removal is more complete for Tedlar and Tefzel than Teflon may be attributed to the presence of H in Tefzel (33 at %) and Tedlar (50 at %). The AO may attack the H^-, resulting in ejection of HF.

All the observations based on the C1s spectra after AO exposure are consistent with the F1s spectra shown in Figure 5. After AO exposure, the F1s peak for PVF (Tedlar) shown in Figure 5(a) is significantly reduced. Also, both the F1s spectra for PVdF (Tefzel) and PTFE (Teflon) shift to lower BE values and broaden with newly developed low BE shoulders as observed in Figure 5(b) and (c). These low BE shoulders formed after AO exposure correspond well with the chemical state of the fluorine found in the preceding polymer of this homologous series when arranged by increasing F : C ratio (Tedlar < Tefzel < Teflon). No specific F1s feature was observed for $–CF_3$ formation in PTFE and reference BE values for this chemical species have not been published in the literature even though $–CF_3$ is found in various polymer films such as Viton, Fomblin Y, and poly-(vinyl trifluoroacetate).

CONCLUSIONS

In this study, a homologous series of fluoropolymers, commonly used in space applications, was characterized with XPS before and after a 15-min exposure to the flux 10^{15} atoms cm^{-2} s^{-1} produced by a unique hyperthermal atomic oxygen source. The linear polymers investigated in this study [high-density polyethylene (HDPE), Tedlar (PVF), Tefzel (PVdF), Teflon (PTFE)] possess a similar base structure with increasing fluorine-to-carbon ratios of 0, 1 : 2, 1 : 1, and 2 : 1, respectively. No interaction of the AO with the nonfluorine-containing linear polymer HDPE was detected for the length of time exposed. A correlation exists between the chemical composition of the fluorinated polymers and the induced chemical and structural alterations occurring in the near-surface region as a result of exposure to AO. The XPS data indicate that AO initially attacks the fluorine portion of the polymers, resulting in a substantial decrease in the near-surface fluorine concentration as observed through lower binding energy shifts in both high-resolution C1s and F1s spectra. This attack most likely occurs by sputter removal of the F by hyperthermal AO. The near-surface fluorine-to-carbon ratios of Tedlar, Tefzel, and Teflon decreased during the 15-min AO exposure by 68, 39, and 18.5%, respectively.

Support for this research was received from the AFOSR through Grant F49620-01-0338.

References

1. Leger, L. J.; Visentine, J. T. J Spacecraft Rockets 1986, 23, 505.
2. Koontz, S. L.; Leger, L. J.; Visentine, J. T.; Hunton, D. E.; Cross, J. B.; Hakes, C. L. J Spacecraft Rockets 1995, 32, 483.
3. Tennyson, R. C. Can J Phys 1991, 69, 1190.
4. Koontz, S. L.; Leger, L. J.; Rickman, S. L.; Hakes, C. L.; Bui, D. T.; Hunton, D. E.; Cross, J. B. J Spacecraft Rockets 1995, 32, 475.
5. Reddy, M. R. J Mater Sci 1995, 30, 281.
6. Packirisamy, S.; Schwam, D.; Litt, M. H. J Mater Sci 1995, 30, 308.
7. Reddy, M. R.; Srinivasanurthy, N.; Agrawal, B. L. Eur Space Agency J 1992, 16, 193.
8. DeGroh, K. K.; Banks, B. A. J Spacecraft Rockets 1994, 31, 656.
9. Grossman, E.; Lifshitz, Y.; Wolan, J. T.; Mount, C. K.; Hoflund, G. B. J Spacecraft Rockets 1999, 36, 75.
10. Wolan, J. T.; Hoflund, G. B. J Vac Sci Technol A 1999, 17, 662.
11. Gonzalez, R. I.; Phillips, S. H.; Hoflund, G. B. J Spacecraft Rockets 2000, 37, 463.
12. Phillips, S. H.; Hoflund, G. B.; Gonzalez, R. I. Proc 45th Int SAMPE Symp 2000, 45, 1921.
13. Hoflund, G. B.; Gonzalez, R. I.; Phillips, S. H. J Adhes Sci Technol 2001, 15, 1199.
14. DeGroh, K. K.; Gaier, J. R.; Espe, M. P.; Cato, D. R.; Sutter, J. K.; Scheiman, D. A. High Perform Polym 2000, 12, 83.
15. Dever, J. A.; DeGroh, K. K.; Banks, B. A.; Townsend, J. A.; Barth, J. L.; Thomson, S.; Gregory, T.; Savage, W. High Perform Polym 2000, 12, 125.
16. Rasoul, F. A.; Hill, D. J. T.; Forsythe, J. S.; O'Donnell, J. H.; George, G. A.; Pomery, P. J.; Young, P. R.; Connell, J. W. J Appl Polym Sci 1995, 58, 1857.
17. Corallo, G. R.; Hoflund, G. B.; Outlaw, R. A. Surf Interface Anal 1988, 12, 185.
18. Davidson, M. R.; Hoflund, G. B.; Outlaw, R. A. Surf Sci 1993, 281, 111.
19. Outlaw, R. A.; Hoflund, G. B.; Corallo, G. R. Appl Surf Sci 1987, 28, 235.
20. Wisotzki, E.; Balogh, A. G.; Horst, H.; Wolan, J. T.; Hoflund, G. B. J Vac Sci Technol A 1999, 17, 14.
21. Wisotzki, E.; Hahn, H.; Hoflund, G. B. Trends and New Applications of Thin Films; Horst Hoffman/Trans Tech Publications: Switzerland, 1998; Vol. 181, pp. 277–278.
22. Davidson, M. R.; Hoflund, G. B.; Outlaw, R. A. J Vac Sci Technol A 1993, 11, 264.
23. Gilbert, R. E.; Cox, D. F.; Hoflund, G. B. Rev Sci Instrum 1982, 53, 1281.
24. Savitsky, A.; Golay, M. J. E. Anal Chem 1964, 36, 1627.
25. Gonzalez, R. I.; Viers, B. D.; Phillips, S. H.; Hoflund, G. B. Journal, to appear.
26. Wagner, C. D.; Riggs, W. M.; Davis, L. E.; Moulder, J. F.; Muilenberg, Eds. Handbook of X-ray Photoelectron Spectroscopy; Perkin–Elmer: Eden Prairie, MN, 1979.
27. Hoflund, G. B. In: Handbook of Surface and Interface Analysis: Methods in Peoblem Solving; Rivière, J. C.; Myhra, S., Eds.; Marcel Dekker: New York, 1998; pp. 57–158.
28. Beamson, G.; Briggs, D., Eds. High Resolution XPS of Organic Polymers: The Scienta ESCA300 Database; Wiley: Chichester, 1992; pp. 54, 226–236.